

Microphase separation in nanocomposite gels

Noboru Osaka,¹ Hitoshi Endo,¹ Toshihiko Nishida,¹ Takuya Suzuki,¹ Huan-jun Li,²
Kazutoshi Haraguchi,² and Mitsuhiro Shibayama^{1,*}

¹Neutron Science Laboratory, Institute for Solid State Physics, The University of Tokyo, Tokai, Ibaraki 319-1106, Japan

²Kawamura Institute of Chemical Research, 631 Sakada, Sakura-shi, Chiba 285-0078, Japan

(Received 10 September 2008; published 15 June 2009)

Microphase separation in poly(*N*-isopropylacrylamide)(PNIPA)-clay nanocomposite hydrogels (NC gels) is investigated by means of contrast-variation small-angle neutron scattering (CV-SANS) and dynamic light scattering (DLS). By using CV-SANS, it is revealed that microphase separation occurs in NC gels above the lower-critical solution temperature (LCST) of PNIPA aqueous solutions. The observed partial scattering functions show that only the spatial distribution of PNIPA chains is highly distorted by microphase separation and PNIPA chains are preferentially adsorbed on the clay surfaces, where the PNIPA-rich phase forms nanoscaled bicontinuous structure mediated by the clay particles. Additional DLS measurements for dilute solutions with PNIPA and/or the clay nanoparticles confirm that aggregation of PNIPA above the LCST is dramatically suppressed by addition of clay particles. Based on these observations, we conclude that strong affinity between the polymer and clay has a significant effect on the phase separation in NC gels and allows one to tune the length scale of the phase separation phenomenon by clay concentration.

DOI: 10.1103/PhysRevE.79.060801

PACS number(s): 82.35.Jk, 83.80.Kn, 61.05.fg, 81.07.-b

Incorporating nanoparticles into polymer matrix is an extensive subject in material sciences, since polymer nanocomposites (PNCs) have various advantages in the mechanical properties [1], functional capabilities [2,3], etc. From a fundamental point of view, such a combination of nanoparticles and polymers offers various phase behaviors. For example, polymer matrices swell by simply dispersing the nanoparticles into them [4], although they remain unchanged in some cases [5]. In an enthalpically dominated system, where the polymer chains are strongly adsorbed on the multiple particles, a bridging-induced “network”-like phase is formed [6]. In the case of block-copolymers which undergo microphase separation into spatially periodic mesophases, hierarchically and rigidly ordered structures of the PNCs can be formed by self-assembly of both nanoparticles and block-copolymers [7,8]. Note that some nanoparticles are used as surfactants to stabilize bicontinuous structures in polymeric systems [9,10]. As mentioned above, a new type of phase behaviors is expected for PNCs by utilizing the affinity, or self-assembling nature of nanocomposites, or even by simply dispersing nanoparticles into the matrix.

A polymer gel is a three-dimensional network formed by chemical or physical cross-linking. Due to the connectivity, it shows phase behaviors different from those in bulk melt or in solution. Recently, a new type of nanocomposite hydrogel (NC gel) was synthesized, where poly(*N*-isopropylacrylamide) (PNIPA) acts as a polymer matrix and discotic clay nanoparticles act as multifunctional cross-linkers in aqueous solutions [11]. It shows many novelties about mechanical properties, optical transparency, extent of volume change, etc. It is known that PNIPA in water shows a lower-critical solution temperature (LCST) at ca. 33 °C [12]. The discotic clays are well studied nanocolloids

which have a large aspect ratio (the diameter and the thickness being 20–30 nm and 1 nm, respectively) with anisotropic charge densities (negative charge on the faces and slightly positive charge on the edges). According to the previous studies, it was suggested that each clay platelet in NC gels was covered by a thin polymer layer due to a hydrogen bonding between them [13]. The novel properties of NC gels can be successfully explained by this structure. So far, phase separation in NC gels with different clay concentrations was studied in terms of transmittance change and swelling/deswelling behavior, and it was suggested that the phase separation of PNIPA was controlled (depressed) in NC gels with clay concentration [14]. However, the microstructure of the NC gel above the LCST has not been elucidated. Therefore, we will present in this Rapid Communication how the affinity between the PNIPA and the clay particles influences the phase separation of the gels depending on the clay concentration by means of contrast-variation small-angle neutron-scattering (CV-SANS) measurements.

NC gels were synthesized by *in situ* free radical polymerization of *N*-isopropylacrylamide (NIPA) monomer in the presence of the synthetic clay Laponite XLG ($[\text{Mg}_{5.34}\text{Li}_{0.660}\text{Si}_8\text{O}_{20}(\text{OH})_4]\text{Na}_{0.660}$) by using potassium peroxodisulfate and *N, N, N', N'*-tetramethylethylenediamine as initiator and catalyst, respectively. The details of sample preparation are described elsewhere [13]. In this study, the NC gels were prepared with keeping the same NIPA content ($C_{\text{NIPA}}=1.0$ M), and the clay concentration, C_{clay} , was varied from 0.02 up to 0.20 M. Hereafter, the clay concentration in NC gels is abbreviated as NC x , where x is $C_{\text{clay}}[\text{M}]\times 100$, e.g., NC15 gels mean the clay content with $C_{\text{clay}}=0.15$ M.

Small-angle neutron scattering (SANS) measurements were conducted at SANS-U diffractometer of the University of Tokyo located at JRR-3 research reactor of Japan Atomic Energy Agency in Tokai, Japan. The incident wavelength was 7.0 Å and the wavelength distribution was ca. 10% [15].

*<http://shibayama.issp.u-tokyo.ac.jp/shibayama/sibayama@issp.u-tokyo.ac.jp>

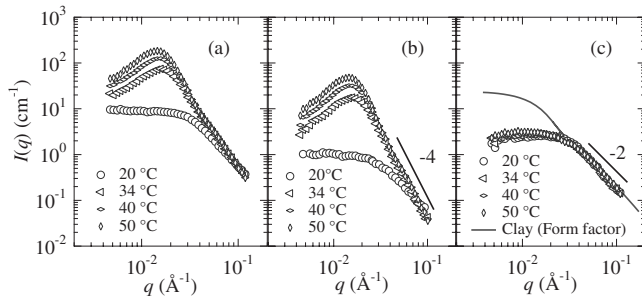


FIG. 1. Scattering curves of NC15 gels showing temperature dependence of NC gels with three different solvent compositions, $\phi_{D_2O}=(a)1.00$, (b) 0.660 (close to clay matching point), and (c) 0.216 (polymer matching point). The solid curve in (c) represents the form factor of the disk-shaped clay particles.

In the case of NC gels, on the incompressibility assumption, the scattering intensities can be described with partial scattering functions (PSFs) $S_{ij}(q)$ as follows,

$$I(q) = \Delta\rho_p^2 S_{pp}(q) + 2\Delta\rho_p \Delta\rho_c S_{pc}(q) + \Delta\rho_c^2 S_{cc}(q), \quad (1)$$

where q is the scattering wave number. $S_{pp}(q)$ and $S_{cc}(q)$ are the self-terms of polymers and clays, respectively, and $S_{pc}(q)$ is the cross term reflecting the cross-correlation between polymers and clays in NC gels. $\Delta\rho_i$ is the scattering contrast between the component i and solvent, where $i=p$ or c indicates polymers and clays, respectively.

The scattering length density of the aqueous solution can be easily tuned by varying the volume fraction of deuterium oxide, ϕ_{D_2O} . We carried out CV-SANS experiments with three different scattering length densities of the aqueous solutions, i.e., $\phi_{D_2O}=1.00$, 0.660 (close to the clay matching point), and 0.216 (close to the polymer matching point) [16]. Then, the obtained intensities were uniquely decomposed into the PSFs according to Eq. (1). The temperature-induced phase separation of NC gels was investigated at 20, 34, 40, and 50 °C for each sample. It is known that deuterium substitution of aqueous solution affects the LCST of NIPA gels [17]. CV-SANS is only applicable to the systems having identical structure. Therefore, we applied CV-SANS technique only to SANS experiments at a temperature far above LCST, i.e., at 50 °C, where the structure difference due to isotope effect was negligible. The aggregation behavior of PNIPA above the LCST in dilute aqueous solutions with or without the clay nanoparticles was also studied by dynamic light scattering (DLS) with an ALV5000 static/dynamic (SLS/DLS) apparatus, ALV, Germany, at a fixed scattering angle of 90°.

Figure 1 shows the temperature dependence of the scattering intensities for NC15 gels ($x=15$) consisting of different D_2O concentrations, ϕ_{D_2O} . Figure 1(a) exhibits the scattering curves with $\phi_{D_2O}=1.00$, which include the contribution of all the PSFs, $S_{pp}(q)$, $S_{pc}(q)$, and $S_{cc}(q)$ in Eq. (1). At 20 °C, which is below the LCST of PNIPA, no characteristic peak was observed in the scattering curve. However, at 34 °C, which is above the LCST, a scattering peak appeared around at $q \sim 0.015 \text{ \AA}^{-1}$, which gradually shifts to the lower q by further heating. This suggests the occurrence

of microphase separation in the NC gels with a Bragg's spacing, d_{Bragg} , of about 420 Å. The physical origin of the peaks is explored in detail by using contrast matching and CV-SANS methods.

Figure 1(b) shows temperature dependence of the scattering intensities of NC15 gels with $\phi_{D_2O}=0.660$ where the clay structure is less visible. A similar temperature dependence of the scattering curves as shown in Fig. 1(a) is observed, which means that PNIPA undergoes microphase separation. The peak positions in Fig. 1(b) are roughly the same as those in Fig. 1(a). In a high q region, the scattering curves superimpose each other with an asymptotic q^{-4} behavior, indicating a formation of sharp boundary in the microphase structure (Porod's law) [18].

Figure 1(c) shows temperature dependence of the scattering intensities of NC15 gels with $\phi_{D_2O}=0.216$, where the polymer is invisible and the clay structure is exclusively observed. Quite interestingly, the scattering curves do not change at all irrespective of temperature. This result means that neither interclay distance nor clay orientation was distorted by microphase separation. The solid curve in Fig. 1(c) represents the form factor of disk-shaped clay particles in the absolute intensity scale. As shown in the figure, the observed scattering intensity is significantly suppressed at low q region in comparison with the calculated form factor. This suppression is due to a repulsive interparticle interaction between clay platelets, which means that they do not aggregate. In addition, the fact of the asymptotic q^{-2} behavior at high q region means that the clays are dispersed randomly in the gels.

From the above arguments, it is conjectured that the microphase separation observed in Fig. 1(a) originates from aggregation of the PNIPA chains, while it does not influence the orientation and the interparticle distance of the clay particles. For further analysis of the PNIPA structure above the LCST, we derived the PSFs of polymer-clay cross term, $S_{pc}(q)$, at 50 °C by using CV-SANS, which was obtained by the decomposition of the three different scattering intensities with different D_2O volume fractions, i.e., $\phi_{D_2O}=1.00$, 0.660, and 0.216, as shown in Fig. 1 into the PSFs. The details of the procedure are described elsewhere [13].

Figure 2 shows the decomposed PSFs of the self-term, the polymer-polymer $S_{pp}(q)$, and the clay-clay $S_{cc}(q)$, as well as the cross term, polymer-clay $S_{pc}(q)$, at 50 °C. The shapes of the $S_{pp}(q)$ and $S_{cc}(q)$ were very similar to the corresponding scattering intensities with $\phi_{D_2O}=0.660$ and 0.216, respectively. Hirokawa *et al.* [19] investigated phase separated structures of a PNIPA gel cross-linked with organic molecules. It was revealed by laser scanning confocal microscopy (LSCM) that there was a micron-order bicontinuous structure in a PNIPA gel. As shown in Fig. 2 (inset), the Fourier transformed image (solid circles) of the LSCM result is quite similar to $S_{pp}(q)$ of NC15 (open circles). Therefore, it is considered that the PNIPA in the NC gels also form a bicontinuous structure, although the scale of the phase separation in NC gels is about 100 times smaller.

$S_{pc}(q)$ in Fig. 2 also has a peak ($q \sim 0.0146 \text{ \AA}^{-1}$), which appears at the same position as that of $S_{pp}(q)$. This suggests that the characteristic distance of polymer-clay is the same as that of polymer-polymer. As a matter of fact, $S_{pc}(q)$ can be

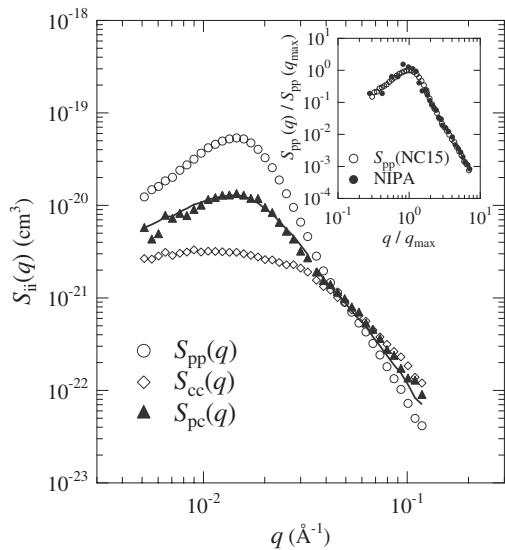


FIG. 2. PSFs for NC15 gels of the self-terms, $S_{pp}(q)$ and $S_{cc}(q)$, and the cross term, $S_{pc}(q)$, at 50 °C decomposed from the scattering curves in Fig. 1. The solid curve is the square root of the product of $S_{pp}(q)$ and $S_{cc}(q)$. Inset: comparison of scaled scattering curves $S_{pp}(q)/S_{pp}(q_{max})$ vs q/q_{max} between NC15 gels (this study) and PNIPa gels (obtained by Fourier transform of the LSCM image and reproduced from Ref. [19]).

well reproduced by the square root of the product of $S_{pp}(q)$ and $S_{cc}(q)$, as shown by the solid curve in Fig. 2, which indicates that the polymers and the clays are strongly correlated. Moreover, it is noteworthy that the $S_{pc}(q)$ has a positive sign in this q region. These experimental results suggest that a significant amount of the PNIPa was adsorbed on the clay surface [13]. In Ref. [20], it was reported that addition of nonionic NIPa monomers to the ionic clay solution decreased the viscosity where the NIPa monomers are adsorbed on the clay surfaces due to hydrogen bonding between NIPa monomer and clay and screened the electrostatic double layer of the clay. Hence, NIPa monomer itself has an attractive interaction with clay. On the other hand, in case of the NC gels, the PNIPa chains have a tendency to aggregate themselves above the LCST [12]. As a result, the aggregated PNIPa chains are preferentially adsorbed on the clay surface. By taking into account of the analogy between NC gel and the LSCM observation of PNIPa gel, it is conjectured that a bicontinuous microdomain structure is formed with polymer-rich network mediated by dispersed clay platelets. The peak shifts toward low q region by increasing temperature shown in Fig. 1(b) is therefore attributed to a deeper phase separation of the bicontinuous structure due to stronger adsorption onto the clay surfaces.

Figure 3 shows the clay concentration dependence of $S_{pp}(q)$ for NC x gels obtained by CV-SANS at 50 °C. The scattering curves are fitted by Teubner-Stern (TS) scattering function which originally represents the scattering curves for bicontinuous structures consisting of oil/water/surfactant microemulsions [21], where $I(q) \sim 1/(a_2 + c_1 q^2 + c_2 q^4)$, with the periodic length $d_{TS} = 2\pi[0.5(a_2/c_2)^{0.5} - 0.25(c_1/c_2)]^{-0.5}$ and the correlation length $\xi_{TS} = [0.5(a_2/c_2)^{0.5} + 0.25(c_1/c_2)]^{-0.5}$. The TS function well reproduces the experimental results

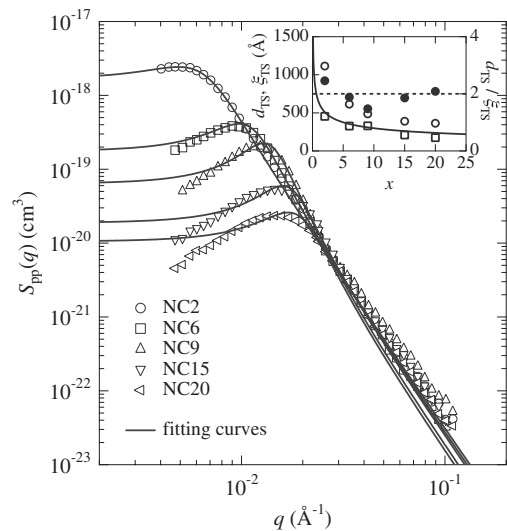


FIG. 3. Clay concentration dependence of $S_{pp}(q)$ obtained by SANS at 50 °C. The solid curves are fitting curves obtained by TS scattering function. Inset: clay concentration dependence of (left) d_{TS} (open circle), ξ_{TS} (open square), and d_{clay} (solid circle), and (right) d_{TS}/ξ_{TS} (solid circle). The broken line represents the constant value 2 (right).

except for low q region where the TS function has a tendency to give excess intensities. This may be due to a lower osmotic compressibility of the gels originating from the elasticity of the connectivity inside the gels in comparison with that of microemulsions. From the fitting, we can estimate d_{TS} and ξ_{TS} , which are shown in the inset of Fig. 3. The periodic length, d_{TS} , was tuned from 360 Å (at $x=20$) to 1110 Å (at $x=2$) by changing the clay content, i.e., x . Note that $d_{TS}=390$ Å (at $x=15$) is close enough to the value of $d_{Bragg}=420$ Å (at $x=15$). In addition, the value of d_{TS}/ξ_{TS} does not depend on x and is rather a constant around 2. This is characteristic of bicontinuous structures [22]. The clay-clay distance, d_{clay} , for random dispersion in three dimensions is estimated to be $d_{clay}=642x^{-1/3}$ Å. As shown in the inset of Fig. 3, d_{clay} is less than d_{TS} , which also suggests the evidence of the bicontinuous structures where the adjacent clay particles are included together in the polymer-rich phase. It was experimentally observed in this work that the value of d_{clay} keeps close to that of ξ_{TS} . It is noteworthy that the NC gels showed a large volume shrinkage at low clay concentrations (i.e., $x \leq 6$), although they show less volume shrinkage at high clay concentration ($x \geq 15$) due to steric hindrance of clay particles. This may be the reason why a deviation from an asymptotic behavior, $d_{clay} \propto x^{-1/3}$, occurs at low clay concentrations.

The above-mentioned phenomena may be explained in terms of a specific interaction between the clay and the polymer. To clarify the presence of specific interaction between the clay and the PNIPa above the LCST, we investigated temperature dependence of hydrodynamic radius by DLS with three different solutions, i.e., PNIPa (0.03 wt %, $M_w=35$ 000, and $M_w/M_n=1.35$), clay (0.0319 wt %), and a mixture of the PNIPa and the clay at equal molar condition, where the molar ratio of the polymer and the clay was equal to that of NC15 gels. Figure 4 shows temperature depen-

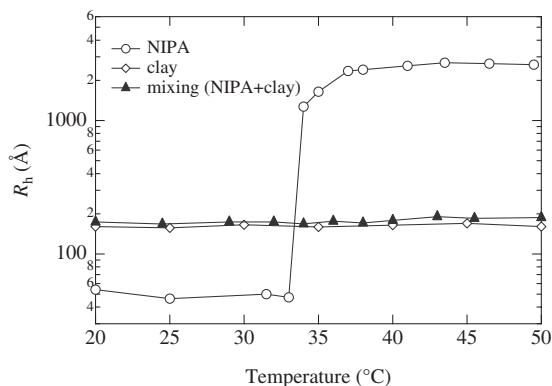


FIG. 4. Temperature dependence of the hydrodynamic radius with three different solutions, 0.03 wt % PNIPA (open circle), 0.0319 wt % clay (open rhombus), and the mixing at equal molar condition (solid triangle).

dence of the hydrodynamic radius obtained by DLS via Stokes-Einstein equation. The obtained hydrodynamic radius of the clay particle was 160 Å and was not dependent on temperature. The hydrodynamic radius of the PNIPA solution, on the other hand, was 54 Å at 20 °C, which is very close to the radius of the single polymer chain. Above the LCST, however, the hydrodynamic radius increased to 2620 Å at 50 °C. This means that the PNIPA chains discontinuously aggregate due to the hydrophobic interaction. On the other hand, the hydrodynamic radius of the mixed solu-

tion was 173 Å at 20 °C, which is almost the same with the clay radius. By heating the solution up to 50 °C, the radius slightly increased up to 188 Å, probably due to local adsorption of PNIPA chains in the vicinity of the clays.

In conclusion, the microscopic structure of the NC gels above the LCST was studied by SANS. Contrast matching SANS confirmed that NC gels undergo microphase separation, where the domain sizes are in the range of several hundred angstroms depending on the clay concentration, while the local structures of clay are unchanged. In addition, CV-SANS clearly showed that the PNIPA chains are strongly adsorbed on the clay particles above the LCST. The specific attractive interaction between the clay and the polymer triggers the phenomenon, which was also confirmed by DLS measurements; i.e., the aggregation size of PNIPA was largely depressed by adding clay particles.

This work was partially supported by the Ministry of Education, Science, Sports and Culture of Japan [Grant-in-Aid for Scientific Research, Grants No. 18205025 and No. 18068004, Grant-in-Aid for Scientific Research (A), 2006–2008, Grant No. 18205025, and for Scientific Research on Priority Areas, 2006–2010, Grant No. 18068004]. The SANS experiment was performed with the approval of Institute for Solid State Physics, The University of Tokyo (Proposals No. 04.041 and No. 04.221), at Japan Atomic Energy Agency, Tokai, Japan.

-
- [1] J. Jordan *et al.*, *Mater. Sci. Eng., A* **393**, 1 (2005).
 [2] R. Gangopadhyay and A. De, *Chem. Mater.* **12**, 608 (2000).
 [3] T. Kashiwagi *et al.*, *Nature Mater.* **4**, 928 (2005).
 [4] M. E. Mackay *et al.*, *Science* **311**, 1740 (2006).
 [5] S. Sen *et al.*, *Phys. Rev. Lett.* **98**, 128302 (2007).
 [6] J. B. Hooper and K. S. Schweizer, *Macromolecules* **40**, 6998 (2007).
 [7] Y. Lin *et al.*, *Nature (London)* **434**, 55 (2005).
 [8] S. W. Sides, B. J. Kim, E. J. Kramer, and G. H. Fredrickson, *Phys. Rev. Lett.* **96**, 250601 (2006).
 [9] H.-j. Chung, K. Ohno, T. Fukuda, and R. J. Composto, *Nano Lett.* **5**, 1878 (2005).
 [10] B. J. Kim *et al.*, *Langmuir* **23**, 7804 (2007).
 [11] K. Haraguchi and T. Takehisa, *Adv. Mater.* **14**, 1120 (2002).
 [12] H. G. Schild, *Prog. Polym. Sci.* **17**, 163 (1992).
 [13] H. Endo *et al.*, *Macromolecules* **41**, 5406 (2008).
 [14] K. Haraguchi *et al.*, *Macromolecules* **40**, 6973 (2007).
 [15] S. Okabe *et al.*, *Nucl. Instrum. Methods Phys. Res. A* **572**, 853 (2007).
 [16] M. Shibayama *et al.*, *Macromolecules* **38**, 10772 (2005).
 [17] M. Shibayama *et al.*, *J. Chem. Phys.* **97**, 6829 (1992).
 [18] O. Glatter and O. Kratky, *Small-Angle X-Ray Scattering* (Academic, London, 1982).
 [19] Y. Hirokawa *et al.*, *Macromolecules* **32**, 7093 (1999).
 [20] K. Haraguchi *et al.*, *Macromolecules* **38**, 3482 (2005).
 [21] M. Teubner and R. Strey, *J. Chem. Phys.* **87**, 3195 (1987).
 [22] T. Sottmann *et al.*, *J. Chem. Phys.* **106**, 6483 (1997).